Journal of Rehabilitation in Civil Engineering 7-2 (2019) 21-39

journal homepage: http://civiljournal.semnan.ac.ir/

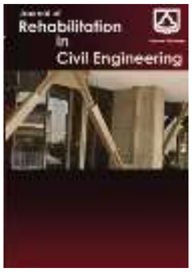

Evaluating the Performance of the Buckling Restrained Braces in Tall Buildings with peripherally Braced Frames

S.A. Seyed Razzaghi[1*] and H.R. Hatami[2]

1. Assistant Professor, Department of Civil Engineering, Payame Noor University, Tehran, Iran
2. M.Sc. of Structural Engineering, Department of Civil Engineering, Payame Noor University, Tehran, Iran

Corresponding author: *arazzaghi@pnu.ac.ir*

ARTICLE INFO

Article history:
Received: 04 September 2017
Accepted: 05 February 2018

Keywords:
High-Rise Buildings,
Buckling Restrained Brace,
Nonlinear Time-Historyanalysis.

ABSTRACT

In recent years, seismic design of structures has been undergoing significant changes as a result of increasing demand for optimization and minimizing the level of damage and reducing the cost of structural repairs, the development of analytical methods and the remarkable improvements of computer performance have been among the factors which influenced the design of structures. A lot of research has been conducted on the development of better braces with perfect elastoplastic behavior. The inventions and development of buckling restrained braces have been the results of these researches. In this study, the performance of Buckling Restrained Environmental Braces (BRB) in high-rise buildings were evaluated applying nonlinear time-history dynamics analysis with three pairs of acceleration and compared with conventional concentrically braced frame (CBF). The studied structures are 20, 40, and 60 stories building which braces were utilized peripherally. The acquired results reveal that the application of Buckling Restrained Brace Frames (BRB) instead of conventional braces frame (CBF) in high-rise steel buildings ameliorates hysteresis behavior of the braces and reduces lateral displacements and increase the capacity of base shear as well.

1. Introduction

The Northridge earthquakes in 1994 revealed the vulnerability of steel moment-resisting frame to several damage related with large displacements. In order to tackle such a problem, engineers are increasingly turning to concentrically brace frames as solution of augmenting the lateral strength and stiffness of steel buildings with the purpose of minimizing the lateral effect of wind and

DOI: 10.22075/JRCE.2018.12407.1213

earthquake, notwithstanding conventional bracing system have performed poorly since compression and tension strengths are unequal as a result ro local buckling and fracture in compressional components which cause less energy dissipation in structural system. The disadvantage of the CBF system can be overcome by boosting dissipation of seismic energy in the system by achieving ductile behaviour. In last decades high number of studies have conducted by researchers and various solutions are introduced to ameliorate bracing system performance. The chevron braced frames seismic performance can be enriched by redesigning the brace and floor beams to the strong beam and a weak brace system. Well hysteretic response acquired in this improved chevron braced frame [1]. An improved balanced design procedure was developed based on the concept of balancing the yield mechanisms and failure modes of the critical elements of the structural system [2]. Yang et al. proposed a method for zipper braced frames designing in order to achieve good ductile behaviour. The zipper braces activated buckling in all storeys except the top one [3, 4]. Moreover, Nouri et al. inspected on the concentric braced frames and employed zipper braced to reduce the vertical unbalanced force in chevron braced frame [5] knee bracings, have also been suggested to ameliorate ductility and attain more efficient damping applying bending and shear yield mechanisms [6-7].

Also Methods such as utilizing Passive energy dissipators including hysteretic or viscoelastic dampers are introduced [8-10]. Employing ductile components in some point of structure is one of the other attempts for dissipating earthquake energy in bracing system [11-14]. The main advantage of using dampers or ductile elements is the absorption of earthquake energy in a separate component of the frame structure. This will reduce the damage of the main structure during the earthquake. Hysteresis dampers have a particular importance as a result to their low cost, high reliability, lack of mechanical components. Buckling restrained braces as a relatively new passive control system has developed to overcome disadvantages of CBF by providing yielding situation for brace elements both in compression and tension without buckling [15-16]. Buckling restrained brace are widely applied in seismic design and retrofitting of buildings especially in the United States and Japan. The effective utilization of buckling restrained brace enhances the performance of structural system under severe earthquake [17]. The main component of BRBs (Fig. 1) consists of a ductile steel section confined by a steel tube filled with a concrete-like material in which a bond-preventing layer decouples the casing from the core so that the brace can slide without interaction with respect to the concrete-filled tube. The main load resisting element in BRB is the steel core that its cross-sectional area can be significantly lower than that of regular braces, due to its unlimited performance caused by buckling. BRBs can absorb significant amount of energy during cyclic loadings because of achieving a high level of ductility and stable hysteresis loops. Experimental results prove the ductile, stable and repeatable hysteretic behaviour of structures utilized with BRBs [18-20]. Furthermore, various studies on the retrofitting and seismic design of structures applying buckling restrained braces developed by researchers [21-25]. Most of above mention studies on the BRBs focused on single bay frames or 2D steel frame structures, so there is scope to inspect implementation of BRBs on real projects having more number of stories with 3D model. In this paper, nonlinear time-history dynamics analysis of a high rise building with dual structural system comprises of moment resisting frame with peripherally brace frames for three pairs of 20, 40, and 60 story buildings is carried out. The results are contemplated in terms of joint displacement, base shear reaction, modal period

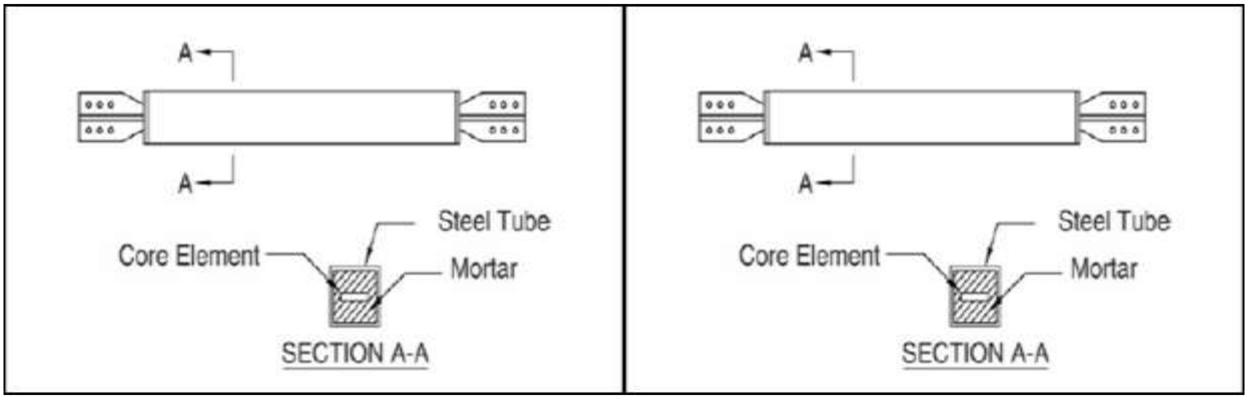

Fig 1. BRB details.

2. Trussed Tube Frames

A tube structure is provided by very stiff frames that form a tube in the perimeter of structure. The peripherally frames include columns spacing from 2 to 4 meters, connected with deep beams. In order to enhance the efficiency of the tube frames, the structural concept based on equivalent tubular system developed by a system of diagonal braces on the exterior frame in which all the exterior columns are fastened by braces and make the whole system behave similar to a rigid box. The essential character of the structure is created by the continuity of the exterior diagonal X-bracing on each face of building. With the exterior trussed-tube assuming all the lateral loads resistance, the interior gravity columns are required to carry only the gravity loads of floors. The lack of internal bracing or other internal lateral resisting elements make it possible to frame floors in a flexible manner in addition to improvement of structural system. . This type of structure was first applied in 1969 for John Hancock Building in Chicago depicted in Figure 2. In the beginning of the project the most important consideration for accepting this diagonally braced truss tube was its efficiency and economy [26]. Structural modeling of 20, 40, and 60 story buildings accomplished by the concept of truss tubular frame in the presented research.

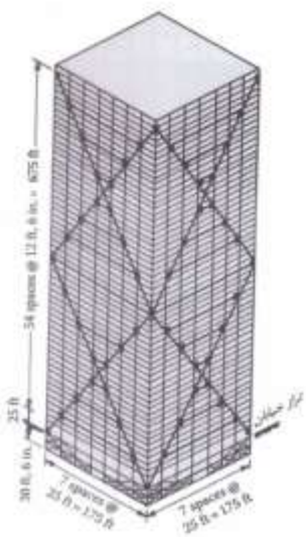

Fig 2. John Hancock's structure with trussed tube frames.

3. Nonlinear Dynamic Time History Analysis

Nonlinear dynamic analysis applies the combination of ground motion records with a detailed structural model; consequently it is capable of fully representing of the seismic response of buildings. In non-linear dynamic analysis, the non-linear characteristic of the structure are contemplated as part of a time domain analysis. This approach is the most rigorous, and is required by some building codes for buildings of uncommon configuration or of special importance. The time history analysis should not be demonstrated with less than three ground motion records (each containing two horizontal components, or if the vertical movement is significant, two horizontal components and a vertical component), and the earthquake records in terms of magnitude, distance from the faults and the source function should be compatible with the site condition. For each category, root sum squares of the 5 percent damped, spectral response from scaled horizontal components of acceleration records requires to be derived.

4. Structural Models and Analysis

This study is concerns about comparative study between similar buildings with BRB and conventional bracing systems. The examined structures are three pairs of 20, 40, 60 story buildings with residential usage. The trussed tubular frames comprises of moment resisting frame with a concentrically brace in perimeter of the structure is contemplated as lateral resisting system. Each one of structures are design with conventional bracing system and buckling restrained braces, the height of all floors is equal to 3.5 meters and the area of each floor is 625 square meters. The diaphragm is considered rigid and stiffness of the braces and the stiffness of floors were considered equal. In this research, the SAP2000-V16 software was utilized based on the 4th edition of the 2800 regulations and the AISC-360-10 code for designing the structures. The structures are assumed to be located in a zone with a high relative seismic hazard based on Iran's 2800 standard and soil type is known as of type III [27]. On that account, the base design acceleration ratio is 0.35g for 475 year return period. In this research, nonlinear dynamic analysis (time history) has been applied as a result to the high rise feature of Buildings. PERFORM 3D software as one of the most fitting software for nonlinear analysis and accurate modeling of BRB is employed.. Tables 2 and 1 reveal the detailed characteristics of materials and gravity loading. The CBF braces are designed applying the strength design method and the relative displacement control. The BRB braces design were based on the Parallel Systems, so the main structural system should be remained in the elastic, the essential factor to be controlled is the slenderness of braces. The slenderness ratio for element in compression should not exceed 6025 /($\sqrt{Fy}$). In table 3 and 4, the property of the sections for columns, beams and braces are presented. Fig. 3, demonstrate the plan and the three-dimensional view of the structures and the location of the braces.

Table 1. Characteristics of materials.

Ec(Kg/cm²)	Fy(Kg/cm²)	Fu(Kg/cm²)
2.1 E 6	2400	3600

Table 2. Gravity loads on buildings.

Situation	Dead load (Kg/m²) (Kg/m)	Live load (Kg / m²)
Floor bottom	600	200
Roof bottom	150	200
Stair bottom	600	350
Unplugged side walls	800	....
side walls with openings	650	....

Table 3. Dimensions of brace elements for BRB and CBF.

		20 floors		
Floor number	5-1	10-6	15-11	20-16
Section CBF	PIP300×15mm	PIP250×12mm	PIP200×10	PIP15×8mm
Section BRB	PIP200×10mm	PIP150×10mm	PIP150×8	PIP10×8mm
		40 floors		
Floor number	1-10	11-20	21-30	31-40
Section CBF	PIP500×15	PIP450×12mm	PIP350×12mm	PIP250×10mm
Section BRB	PIP400×12	PIP350×10mm	PIP300×10mm	PIP200×6mm
		60 floors		
Floor number	15-1	30-16	45-31	60-46
Section CBF	PIP600×25mm	PIP500×15	PIP450×12mm	PIP350×12mm
Section BRB	PIP500×20mm	PIP400×12	PIP350×10mm	PIP300×10mm

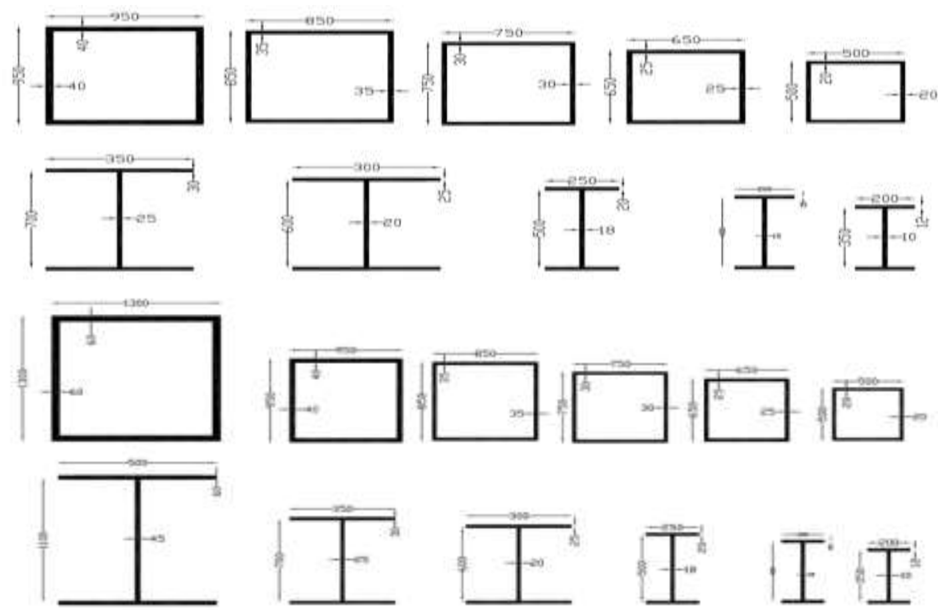

Fig. 3. Dimensions of columns and steel beams used for buildings of 20, 40, 60 floors.

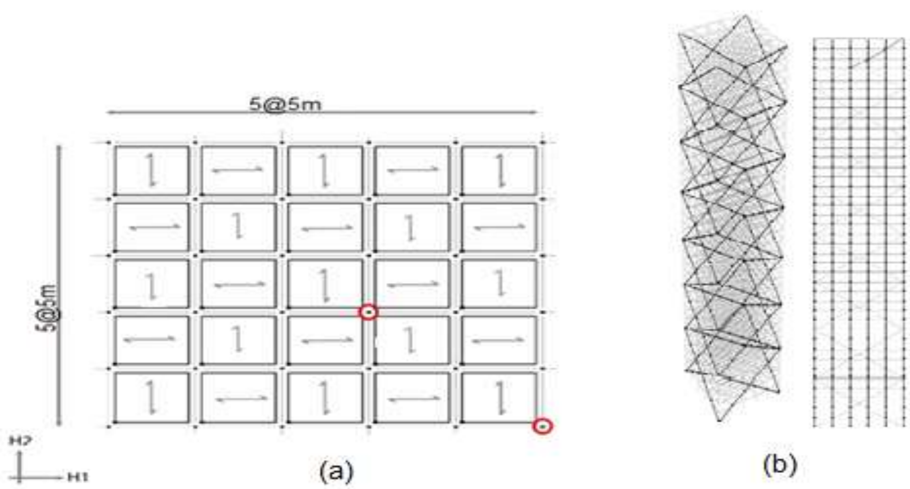

Fig 4. a) Plan and b) structure model of the buildings with 20, 40, 60 floors.

5. Selecting of Acceleration

The selection of seismic motions is one of the most discussed issues for the time-history analysis. In this research, 3 pairs of acceleration records of Kobe, Tabas and Cape Mendocino earthquakes are employed contemplating near fault effect.. The seismological properties of the records applied for this study are summarized in in Table 5. The distances from the sources for the records used to carry the inelastic analyses range between 6 to 10 kilometers the above suite of strong motions covers a range of design scenario for near fault earthquake. Noting that Forward rupture directivity causes the horizontal strike-normal component of ground motion to be systematically larger than the strike-parallel component.

Table 5. Accelerations used in nonlinear dynamic analysis.

Row	Earthquake	Year	Station	Amount Mw)(	PGA (g)	PGV (cm/s)
1	Cape Mendocino	1978	Petrolia	7.1	0.66	89.68
2	Tabas	1979	Tabas	7.4	0.836	97.8
3	Kobe	1995	Takatori	6.9	0.611	127.1

6. Modeling Software

The studied structures were modeled and loaded in the Sap2000 software and consequently dynamic linear time-history Design of structural members is conducted based on AISC-360-10 and 2800 standard. In order to avoid buckling, the unbraced Length Ratio of BRB members were contemplated to be small amount equal to 0.01. Over the past decades, researchers have been developing seismic design concepts based on performance. Performance levels were expressed as acceptable levels of damage categorized as Immediate Occupancy, Life Safety and Collapse Prevention. This approach is generally developed for evaluation and retrofitting process of existing buildings. In order to apply performance based design concepts in estimating the performance of buildings, the PERFORM3D as a finite element software was applied in this project. The software provides performance-based design which is able to compute the demand / capacity ratio for all components in all limit states.. Complex structures including buildings with wide range of variables can be analyzed based on deformation and resistance.

6.1. Beam Elements

In the process of modeling the elements of the beam, all the characteristics of the beams sections including the axial cross section area, the shear cross section along the 2nd and 3rd moment of inertia and the moment of inertia for the 2nd and 3rd direction of the cross section were assigned. [28].

nonlinear characteristics of beam elements are specified by force-deformation relationship, with points Y, U, L and R, in order to capture the main aspects of the nonlinear behavior of beam, namely the initial stiffness, strain hardening, ultimate strength and strength loss, as indicated in the figure5, for a steel beam component, the deformations at points U, L, R, and X are computed based on the deformation at the Y point. [29] In the definition of nonlinear characteristics of beams, the below procedure is followed.

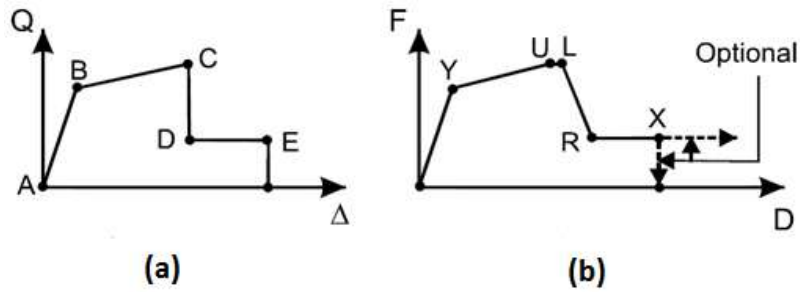

Fig 5. Force-deformation relationship, a. FEMA356, b. PERFORM3D.

The FU value is determined by the relation (1):

$$M_{CE} = Z \times F_{ye} = 1.1 \times Z \times F_y \qquad (1)$$

In the above relation, Z is plastic section modulus and F_{ye} is the expected steel yield stress.

All values for the positive and negative rotations in point X are determined pursuant to Table 6. The tables represent modeling parameters and acceptance criteria for nonlinear methods related to beams [29]

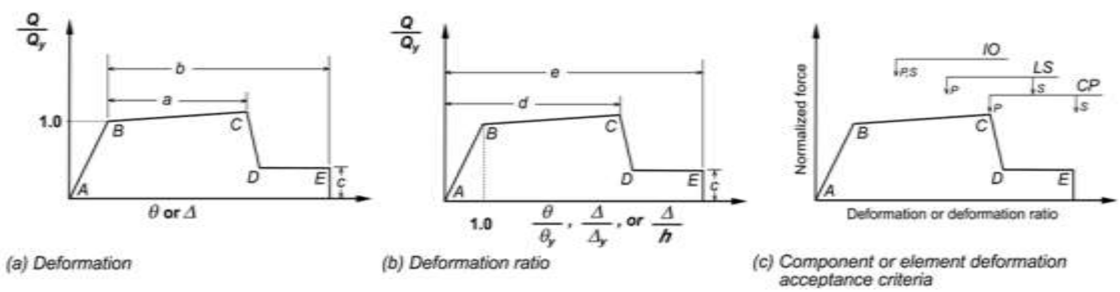

Fig 6. Deformation-force diagram for steel beam (FEMA273, 1997).

Table 6. Modeling parameters and acceptance criteria for steel beams in nonlinear methods.

	Modeling Parameters			Acceptance Criteria				
	Plastic Rotation Angle, Radians		Residual Strength Ratio	Plastic Rotation Angle, Radians				
					Primary		Secondary	
Component/Action	a	b	c	IO	LS	CP	LS	CP
Beams—flexure								
a. $\frac{b_f}{2t_f} \le \frac{52}{\sqrt{F_{ye}}}$ and $\frac{h}{t_w} \le \frac{418}{\sqrt{F_{ye}}}$	$9\theta_y$	$11\theta_y$	0.6	$1\theta_y$	$6\theta_y$	$8\theta_y$	$9\theta_y$	$11\theta_y$
b. $\frac{b_f}{2t_f} \ge \frac{65}{\sqrt{F_{ye}}}$ or $\frac{h}{t_w} \ge \frac{640}{\sqrt{F_{ye}}}$	$4\theta_y$	$6\theta_y$	0.2	$0.25\theta_y$	$2\theta_y$	$3\theta_y$	$3\theta_y$	$4\theta_y$
c. Other	Linear interpolation between the values on lines a and b for both flange slenderness (first term) and web slenderness (second term) shall be performed, and the lowest resulting value shall be used							

6.2. Column Elements

In the process of defining cross-sectionfor columns, all information such as section size, shear area around the local axis 2 and 3, torsional inertia, and other parameters for all column elements are similar with Section 5.1.1.

The PERFORM 3D program is able to compute the shear area around the local axis 2 and 3, the inertia moment, and etc. the values of the expected bending moment and the Expected axial yield force for both tensile and compression loading of the column which are presented in Fig. 7. Meanwhile, the ratio of the axial displacement/expected yield displacement and the ratio of rotation/ expected yield rotation at point X were calculated for the component according to the structure. In determining amount of strength loss, the amount of DL for bending around axes 2 and 3 is contemplated equal to 10 times of the yielding bending deformation as illustrated in Fig. 8. In determining the corresponding bending deformation for each performance level, 1, 2, 7, 9, and 12 is assigned to 1, 2, 3, 4, 5 performance levels respectively which is displayed in Table 7.

In determining the corresponding

Table 7. Modeling parameters and acceptance criteria for steel columns in nonlinear methods.

	Modeling Parameters			Acceptance Criteria				
	Plastic Rotation Angle, Radians		Residual Strength Ratio	Plastic Rotation Angle, Radians				
					Primary		Secondary	
Component/Action	a	b	c	IO	LS	CP	LS	CP
Columns—flexure [2, 7]								
For $P/P_{CL} < 0.20$								
a. $\frac{b_f}{2t_f} \le \frac{52}{\sqrt{F_{ye}}}$ and $\frac{h}{t_w} \le \frac{300}{\sqrt{F_{ye}}}$	$9\theta_y$	$11\theta_y$	0.6	$1\theta_y$	$6\theta_y$	$8\theta_y$	$9\theta_y$	$11\theta_y$
b. $d\,\frac{b_f}{2t_f} \ge \frac{65}{\sqrt{F_{ye}}}$ or $\frac{h}{t_w} \ge \frac{460}{\sqrt{F_{ye}}}$	$4\theta_y$	$6\theta_y$	0.2	$0.25\theta_y$	$2\theta_y$	$3\theta_y$	$3\theta_y$	$4\theta_y$

6.3. Braces

As we know, braces are members of trussed tube structures that carry the role of bearing lateral forces such as wind and earthquakes. Strut members were applied in this project to model brace elements. For modeling this element, the property of material must be specified.

The nonlinear behavior of the bracing elements depends on the cross-sectional area and the length of the brace element. The tensile strength of the steel under the tensile axial tension is set to $1.1F_y$. Moreover, the ultimate strain of the material is computed pursuant to Table 8 using a steel yield strain under tensile axial tension. The critical stress subjected to compression stress is acquired through equation 2.

$$F_{cr} = \left(0.658^{F_y/F_{ye}}\right)F_y \qquad (2)$$

Which F_y is the steel yield tension obtained by the equation 3. [27]

$$F_{ye} = \frac{\pi^2 E}{(\frac{KL}{r})^2} \quad (3)$$

In which K is effective length factor, whose value depends on how the ends of the element are fixed

Table 8. Modeling parameters and acceptance criteria for braces in nonlinear methods.

	Modeling Parameters			Acceptance Criteria				
				Plastic Deformation				
	Plastic Deformation		Residual Strength Ratio		Primary		Secondary	
Component/Action	a	b	c	IO	LS	CP	LS	CP
Braces in Compression (except EBF braces)[1]								
a. Double angles buckling in-plane	$0.5\Delta_c$	$9\Delta_c$	0.2	$0.25\Delta_c$	$5\Delta_c$	$7\Delta_c$	$7\Delta_c$	$8\Delta_c$
b. Double angles buckling out-of-plane	$0.5\Delta_c$	$8\Delta_c$	0.2	$0.25\Delta_c$	$4\Delta_c$	$6\Delta_c$	$6\Delta_c$	$7\Delta_c$
c. W or I shape	$0.5\Delta_c$	$8\Delta_c$	0.2	$0.25\Delta_c$	$5\Delta_c$	$7\Delta_c$	$7\Delta_c$	$8\Delta_c$
d. Double channels buckling in-plane	$0.5\Delta_c$	$9\Delta_c$	0.2	$0.25\Delta_c$	$5\Delta_c$	$7\Delta_c$	$7\Delta_c$	$8\Delta_c$
e. Double channels buckling out-of-plane	$0.5\Delta_c$	$8\Delta_c$	0.2	$0.25\Delta_c$	$4\Delta_c$	$6\Delta_c$	$6\Delta_c$	$7\Delta_c$
f. Concrete-filled tubes	$0.5\Delta_c$	$7\Delta_c$	0.2	$0.25\Delta_c$	$4\Delta_c$	$6\Delta_c$	$6\Delta_c$	$7\Delta_c$
g. Rectangular cold-formed tubes								
1. $\frac{d}{t} \le \frac{90}{\sqrt{F_y}}$	$0.5\Delta_c$	$7\Delta_c$	0.4	$0.25\Delta_c$	$4\Delta_c$	$6\Delta_c$	$6\Delta_c$	$7\Delta_c$
2. $\frac{d}{t} \ge \frac{190}{\sqrt{F_y}}$	$0.5\Delta_c$	$3\Delta_c$	0.2	$0.25\Delta_c$	$1\Delta_c$	$2\Delta_c$	$2\Delta_c$	$3\Delta_c$
3. $\frac{90}{\sqrt{F_y}} \le \frac{d}{t} \le \frac{190}{\sqrt{F_y}}$	Linear interpolation shall be used.							
Braces in Tension (except EBF braces)[2]	$11\Delta_T$	$14\Delta_T$	0.8	$0.25\Delta_T$	$7\Delta_T$	$9\Delta_T$	$11\Delta_T$	$13\Delta_T$

The composite component of BRB is an axial component that only deal with axial forces and torsional and flexural stiffness is assumed to be zero. In fact, instead of modeling each of the three components of BRB: a steel core that sustains axial inelastic deformations in tension and compression, a split glulam casing providing buckling restraint, and a deboned interface (air gap) between the casing and core plate that allows for relative movement of the components along the axis of the brace, force-displacement diagram of considered composite element are applied to model it. 30% of the buckling restrained length of the brace is contemplated to be the end zone. Figure 9 illustrates the load-displacement curve of the buckling restrained braces, taking into account that R_y = 1.1, ω = 1.25 and β = 1.1. So that R_y is the over strength factor, ω is the strain-hardening coefficient and β is the compressive strength coefficient [30].

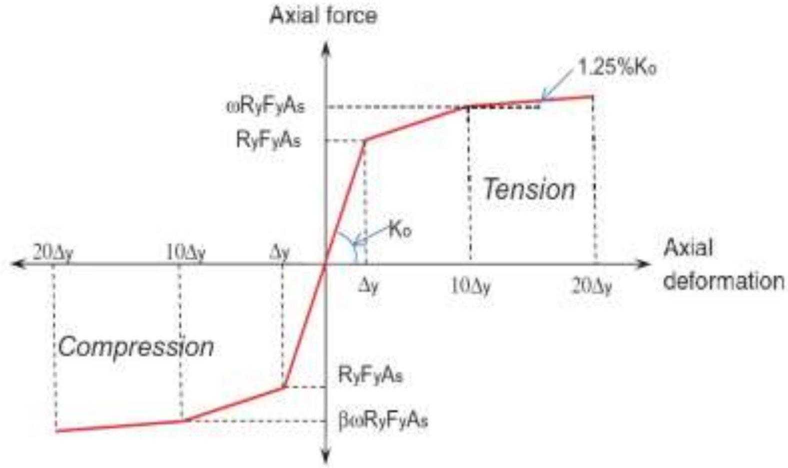

Fig 9. load-displacement curve for the BRB element.

Considering that the nonlinear behavior of the bracing elements BRB depends mostly on the cross-section of the brace element in agreement to the criteria in Table 9. So, for each braces applied in models with different sections and lengths, a buckling resisted material was defined. For modeling the nonlinear behavior of BRB braces, the Basic Components = Buckling Restrained Brace + Elastic Bar have been used to model the Compound in BRB braces

Table 9. Modeling parameters and acceptance criteria for BRB braces in nonlinear methods.

	Modeling Parameters			Acceptance Criteria		
	Plastic Deformation		Residual Strength Ratio	Plastic Deformation		
Component/Action	a	b	c	IO	LS	CP
Braces in Tension (except EBF braces)[f,g]						
1. W	$10\Delta_T$	$13\Delta_T$	0.6	$0.5\Delta_T$	$10\Delta_T$	$13\Delta_T$
2. 2L	$9\Delta_T$	$12\Delta_T$	0.6	$0.5\Delta_T$	$9\Delta_T$	$12\Delta_T$
3. HSS	$9\Delta_T$	$11\Delta_T$	0.6	$0.5\Delta_T$	$8\Delta_T$	$11\Delta_T$
4. Pipe	$8\Delta_T$	$9\Delta_T$	0.6	$0.5\Delta_T$	$7\Delta_T$	$9\Delta_T$
5. Single angle	$10\Delta_T$	$11\Delta_T$	0.6	$0.5\Delta_T$	$8\Delta_T$	$10\Delta_T$
Beams, columns in tension (except EBF beams, columns)[e]	$5\Delta_T$	$7\Delta_T$	1.0	$0.5\Delta_T$	$6\Delta_T$	$7\Delta_T$
Buckling-restrained braces[h,i]	$13.3\Delta_y$	$13.3\Delta_y$	1.0	$3.0\Delta_y$	$10\Delta_y$	$13.3\Delta_y$

7. Analysis Results

7.1 Natural Period and Stiffness of Structures

As displayed in Fig. 10, the natural period in a structure applied with BRB brace is more than the CBF brace structure, it can be observed that utilizing BRBs in taller buildings provide longer fundamental period in comparison to CBFs, for instance applying BRBs In the 60 story building make fundamental period become one second longer and the higher amount of period means lower amount of stiffness and more ductility.

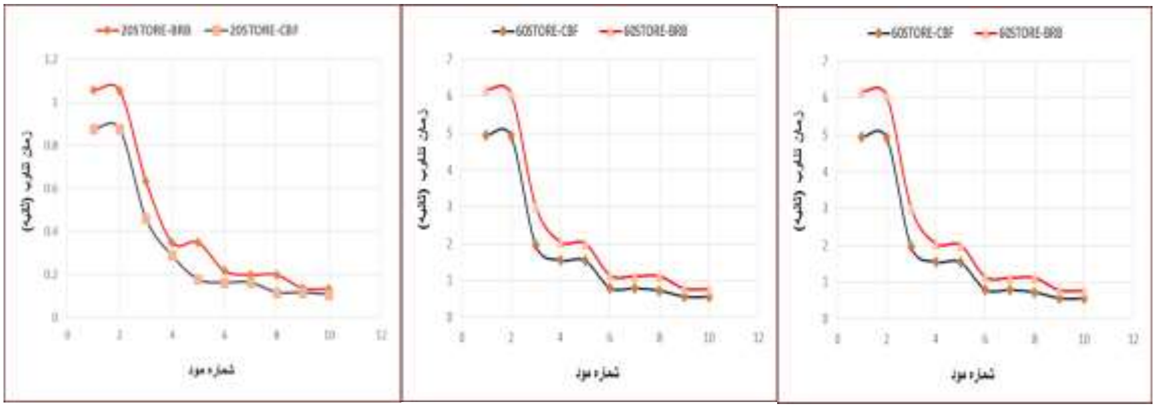

Fig 10. Comparison of the period for structures of 20, 40 and 60 floors.

7.2. Comparison of Lateral Displacement of Floors

One of the crucial factors in structures analysis is the maximum lateral displacement ratio, which is defined as the dissimilarity between the roof and floor displacements of any given story as the building sways during the earthquake, normalized by the story height. The design for drift and lateral stability is an issue that should be addressed in the early stages of design development. In many cases especially in tall buildings or in cases where torsion is a major contributor to structural response, the drift criteria can become a governing factor in selection of the proper structural system. During an earthquake, required inelastic drift in order to prevent the instability and additional effects of P-Δ is limited to amount less than 0.02 [31]. Distribution of inter-story drift ratio (IDR) for each of the horizontal components of motion (H1 and H2) is demonstrated in Figures 11 to 16. e. The maximum amount of the IDR for 20-story building for both H1 and H2 components have observed in the middle floors. The impact of Tabas earthquake on H1 direction and the H2 component of Kobe at were greater than the other earthquakes, notwithstanding IDR does not exceed 0.02, and the BRB utilized structures have more uniform distribution of IDR in comparison to CBF braces This is because of the asymmetric behavior of CBFs elements and occurrence of buckling in the compression components while BRBs still provide stiffness for structure with a symmetric behavior in tensile and compression. The grate changes in IDR for the 40-story building have occurred in the lower floors. The impact of Tabas earthquake on the H1 direction and the Capemendo at H2 direction was more considerable than the other earthquakes, hence that the rate of IDR at both directions does not exceed 0.02. The noticeable changes in the 60-story building have occurred in the high floors. The impact of Tabas earthquake on both H2 and H1 was more severe than other earthquakes, so that the IDR for the H2 direction exceeds 0.02. This indicate that the impact of the Kobe earthquake on short-natural-period buildings response is greater, and by increaseing the height of the building (60-story buildings), Tabas earthquake instead of the Kobe earthquake cause the big amount of IDR.

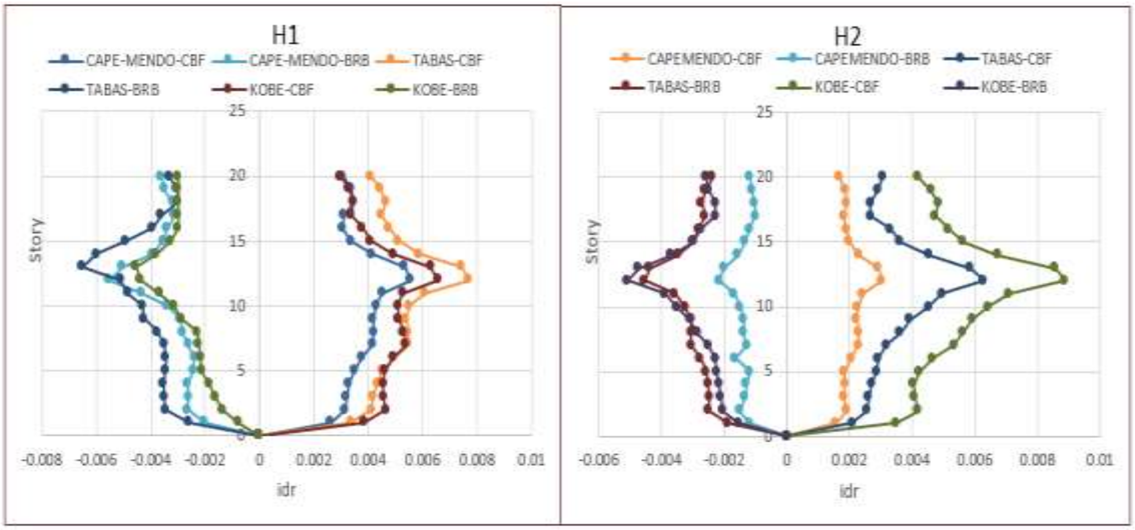

Fig 11. Maximum inter-story drift for the 20-floor building along H1 and H2.

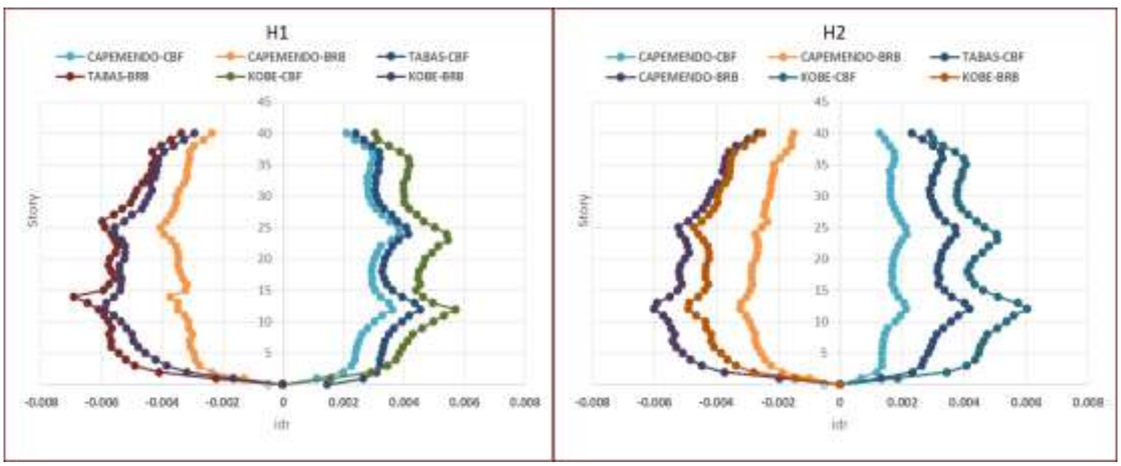

Fig 12. Maximum inter-story drift for 40-floor building along H1 and H2.

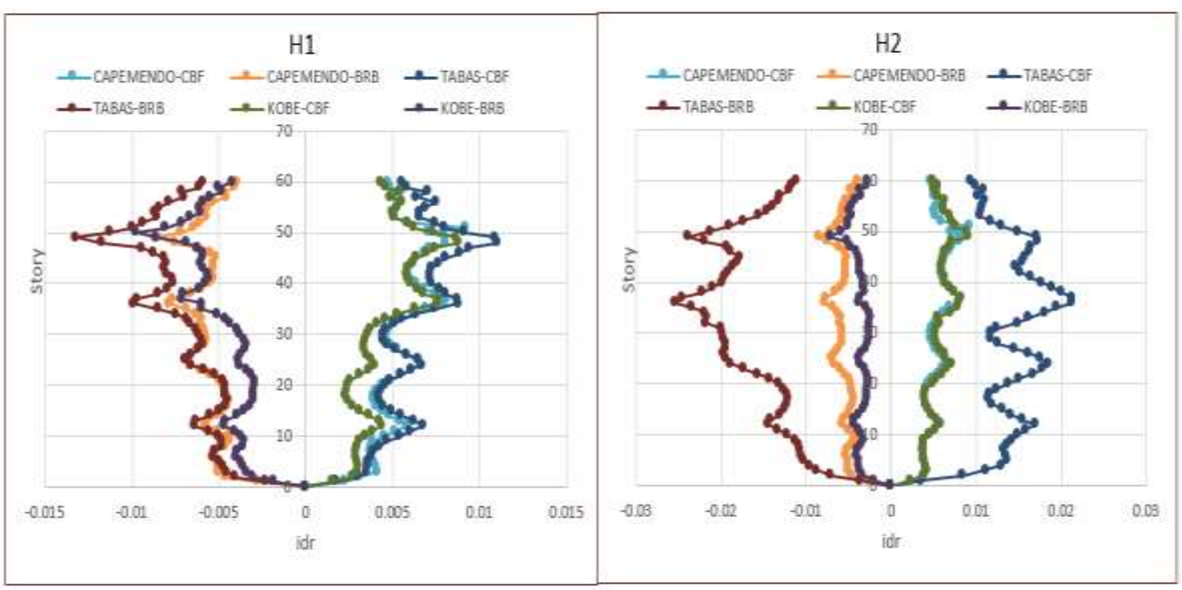

Fig 13. Maximum inter-story drift for 60-floor building along H1 and H2.

7.3. Base Shear

As can be observed in Figures 14-16, comparing the time-history base shear of the buildings 60, 40, and 20-floor revealed that the lateral base shear capacity of buildings equipped with BRB braces is more of certain percentage than CBF buildings. 25% increase in shear capacity observed in the 20 story building under Kobe earthquake and for the 40 story model an increase equal to 30% is computed applying Tabas earthquake and finally for the 60 story building 28% amount of increase is revealed. As it was anticipated BRBs can effectively attract base shear and reduce the force in other structural elements of lateral resisting system. It is noticed that percentage of increase in shear capacity dose not grows for the building higher the 40 story model.

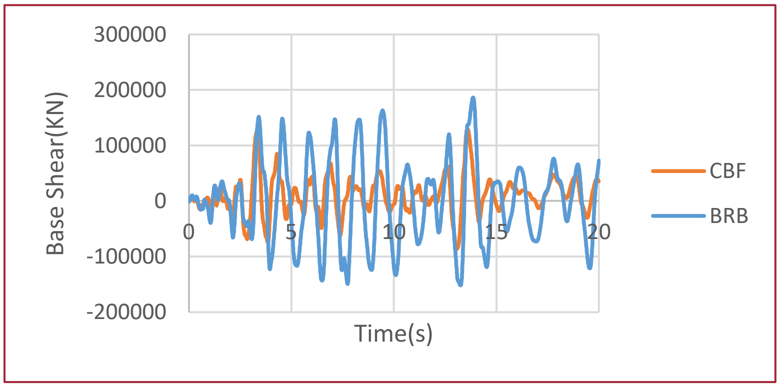

Fig14. Comparison of the time history base shear of the 20-floor building under Kobe earthquake.

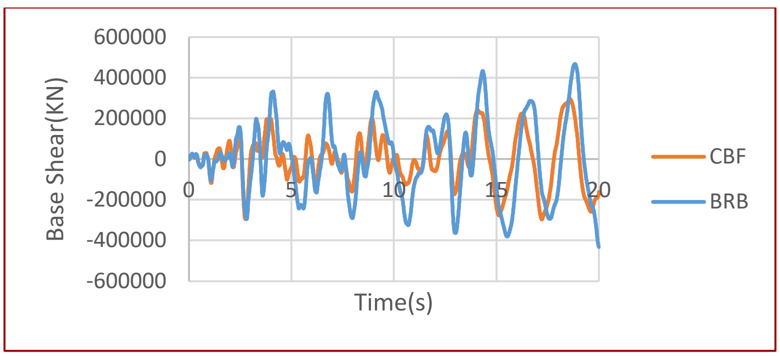

Fig 15. Comparison of the time history base shear for the 40-floor building under Tabas earthquake.

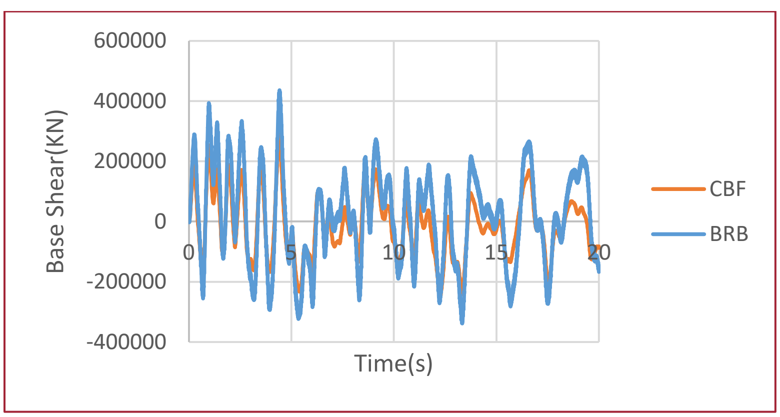

Fig 16. Comparison of the time history base shear for the 60-floor building under Cape Mendocino earthquake.

7.4. Dissipated Energy

evaluate the amount of energy dissipated in the structures, various mechanisms can be applied such as. Here is a diagram of the imposed energy to the structures, using the diagram the amount of energy dissipated by each of the systems can be calculated. As it is revealed, each method is represented by a specific color. As indicated in Figs. 17, Normalized hysteretic energy dissipated by the BRB configurations was greater than those of the CBF configurations. These results again highlight the strong correlation between fatigue life and the effective slenderness ratio of a brace. The concrete and steel tube encasement provides sufficient flexural strength and stiffness to prevent global buckling of the brace, allowing the core to undergo fully reversed axial yield cycles without loss of stiffness or strength. The concrete and steel tube helps to resist local buckling as well. It has been displayed that short-period structures are very sensitive to hysteretic shape during dynamic excitation.

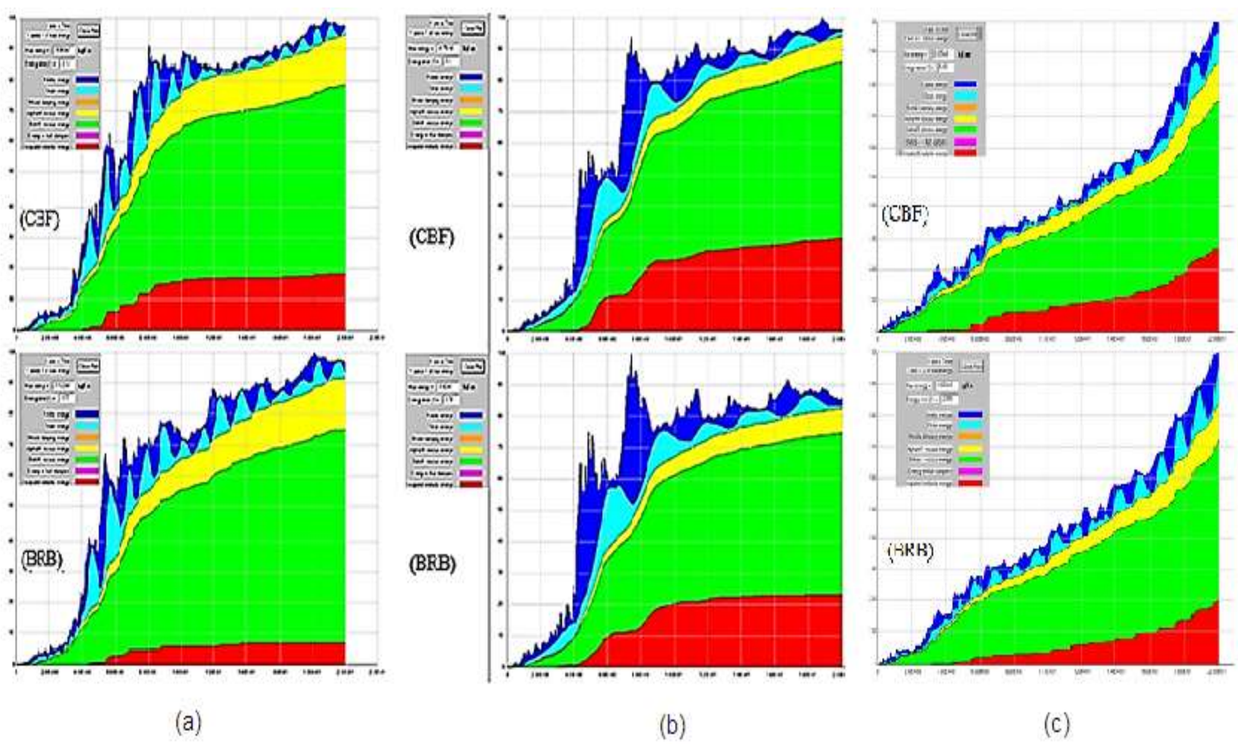

Fig 17. Comparison of energy dissipation in the a) 20, b) 40 and c) 60-story building.

7.5. Hysteresis Behavior

Regarding to figures 18 to 20, the symmetrical hysteresis behavior of buckling restrained braces indicates their high energy absorption capability and the number of complete loading cycles in BRB is more than the typical braces.

One of weaknesses of the typical buckling braces is the dissimilarity between their tensile and compressive strength and, as a result, low resistance of these braces against cyclic loading. However, in the buckling restrained braces, the core must be designed in such a way that it is involved in the surrender both in the compression and tension.

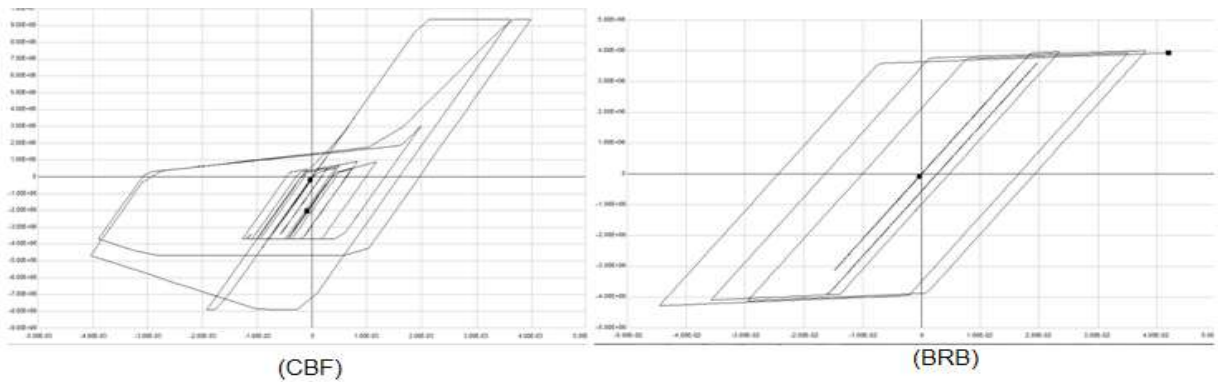

Fig 18. Comparison of CBF and BRB hysteresis behavior in 20-floor building under Kobe earthquake.

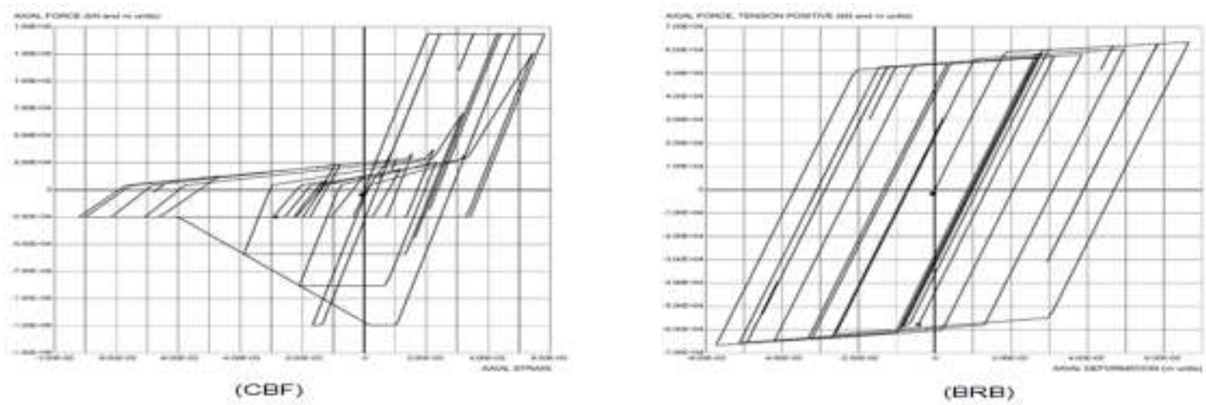

Fig 19. Comparison of CBF and BRB hysteresis behavior in 40-floor building under Kobe earthquake.

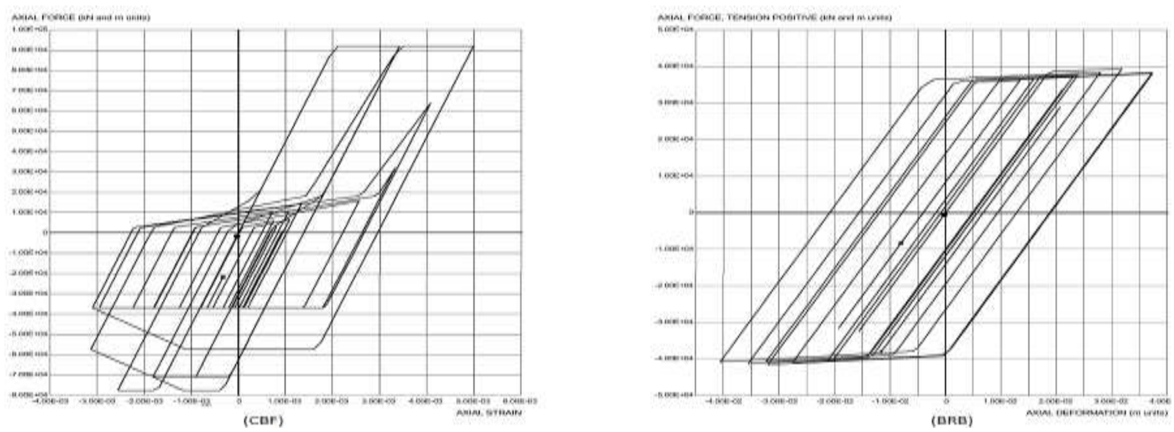

Fig 20. Comparison of CBF and BRB hysteresis behavior in 20-floor building under Kobe earthquake.

8. Conclusion

In this research, the comparison of buckling restrained braces with typical concentrically brace in high-rise steel buildings with a regular plan by dual structural system comprises of moment resisting frame with a concentrically brace in perimeter was inspected based on non-linear time-history dynamics analysis. To this end, First, sections were designed for modeled structure of 20,40.60 story building applying SAP2000 software based on the 4th edition of the 2800 standard and the AISC-360-10 code, and consequently nonlinear dynamic analysis is conducted in the structures applying PERFORM 3D software under the influence of 3 pairs of accelerations. Cape Mendocino, Tabas, Kobe earthquakes are the earthquakes considered in this study. At last, it was found that applying the peripheral BRB braces in high-rise structures instead of CBF braces has the following results:

-Increasing the natural period of the structure and reducing the structural stiffness by boosting its ductility. The fundamental period of the examined structures increased about 20%.

relative lateral displacement and overall lateral displacement because of symmetric behavior in tensile and compression. Inter-story drift of the 2o story building reduce between approximately 35-50 percent in different stories. It is observed that the maximum ratio of drift occurs in the middle floors despite, its rate in both perpendicular directions does not exceed 0.02. in the 40 story building, Decreasing of the inter-story drift and overall lateral displacement vary from 20 to 35 percent in different stories, and , it is observed that the maximum ratio of drift occurs in the lower floors which are limited to 0.02 in both directions. t in the 60-storey building, the maximum ratio of drift has occurred in the upper floors and its drift ratio in one of directions is more than 0.02.

- The lateral base shear capacity Increase for about 25% to 30% and As it was expected, employing BRBs can effectively attract base shear and reduce the force in other structural elements of lateral resisting system.
- Normalized hysteretic energy dissipated by the BRB configurations is increased for about 20% to 30% minimizing damages in main elements of structures.
- Ameliorating the symmetrical hysteresis behavior of buckling restrained braces that indicates their ability to absorb more energy. The number of complete load cycles in this type of braces is several times more than the typical braces.

- Either CBF or BRB braces in the examined high-rise buildings with tubular system alone couldn’t satisfy the lateral displacement limitation effectively so applying additional system, such as a shear wall or a truss belt system is inevitable.

REFERENCES

[1] Rai, D.C., Goel, S.C. (2003). Seismic evaluation and upgrading of chevron braced frames, Journal of Constructional Steel Research, 59: 971-994.

[2] Roeder, C.W., Lumpkin, E.J., and Lehman, D.E. (2011). Balanced Design Procedure for Special Concentrically Braced Frame Connections, Journal of Constructional Steel Research (Elsevier), 67(11): 1760-72.

[3] Yang, C.S., Leon, R.T., DesRoches R. (2008). Design and behavior of zipper braced frames, Engineering Structures, 30: 1092-1100.

[4] Yang, C.S., Leon, R.T., DesRoches R. (2008). Pushover response of a braced frame with suspended zipper struts, Journal of Structural Engineering (ASCE), 134(10):1619-1626.

[5] Nouri, G.R., Kalesar, H.I., Ameli, Z. (2009). The applicability of the zipper strut to seismic rehabilitation of steel structures, World Academy of Science, Engineering and Technology, 58: 402-405.

[6] Naeim F. (2002). The Seismic Design Handbook, Second Edition, New Jersey: Prentice-Hall.

[7] Aristizabal-Ochoa J. D. (1986). Disposable knee bracing: improvement in seismic design of steel frames, Journal of Structural Engineering, 112: 1544–1552.

[8] Constantinou, M. C., Tsopelas, P., Hammel, W., and Sigaher, A. N. (2001). Toggle-brace-damper seismic energy dissipation systems, J.Struct. Eng., 127(2): 105–112.

[9] Ibrahim, Y. E., Marshall, J., and Charney, F. A. (2007). Avisco-plastic device for seismic protection of structures, Journal of Constructional Steel Research, 63: 1515-1528.

[10] Hanson, R. D. and Soong, T. T. (2001). Seismic design with supplemental energy dissipation devices. Earthquake Engineering Research Institute,Oakland, C.A., USA

[11] Bazzaz M., Andalib Z., Kheyroddin A. and Kafi M.A. (2015). Numerical Comparison of the Seismic Performance of Steel Rings in Off-centre Bracing System and Diagonal Bracing System, Journal of Steel and Composite Structures, 19(4): 917-937.

[12] Bazzaz M., Andalib Z., Kafi M.A. and Kheyroddin A. (2015). Evaluating the Performance of OBS-C-O in Steel Frames under Monotonic Load, Journal of Earthquakes and Structures, 8(3): 697-710.

[13] Andalib Z., Kafi M.A., Kheyroddin A. and Bazzaz M. (2014). Experimental Investigation of the Ductility and Performance of Steel Rings Constructed from Plates, Journal of Constructional steel research, 103:77-88.

[14] Bazzaz M., Kheyroddin A., Kafi M.A., Andalib Z. and Esmaeili H. (2014). Seismic Performance of Off-centre Braced Frame with Circular Element in Optimum Place, International Journal of Steel Structures, 14(2): 293-304.

[15] Wada A., and at el, Development of unbounded brace, Structural Research Center, Tokyo Institute of Technology, Yokohama, Japan.

[16] Wada, A., Huang, Y.H. and Iwata, M. (1999). Passive damping technology for buildings in Japan, Progress in Structure Engineering and Material, 2:1-15

[17] Berkeley, C. A., Dutta, A., and Hamburger, R. O. (2011). Case Study of a 40-Storey Buckling-Restrained Braced Frame Building Located in Los Angeles, The Structural Design of Tall and Special Building (Wiley InterScience), 19: 77-93

[18] Merritt, S., Uang, Ch. M., Benzoni, G. (2003). Subassemblage testing of Star Seismic buckling-restrained braces, Test report, University of California, San Diego.

[19] Newell, J., Uang, Ch.M., Benzoni, G. (2006). Subassemblage Testing of Corebrace Buckling-Restrained Braces (G-Series). Test Report, University of California, San Diego.

[20] Dunai L. (2011). Type testing of Buckling Restrained Braces according to EN 15129 – EWC800 – Final report.

[21] Kim, J., Park, J., Shin, S.W., & Min, K.W. (2009). Seismic Performance of Tubular Structures with Buckling Restrained Braces; The Structural Design of Tall and Special Buildings. Vol. 18, pp: 351-370.

[22] Shadiya, K.P., & Anjusha, R. (2015). Bracing Configurations Effect on Buckling Restrained Braced Frames, International Journal of Innovative Research in Science, Engineering and Technology, Vol. 4, Issue 4.

[23] Eletrabi, H., & Marshall, J.D. (2015). Catenary action in steel framed buildings with buckling restrained braces, Journal of

Constructional Steel Research, Vol. 113, pp: 221–233.

[24] Bazaez, R., & Dusicka, P. (2016). Cyclic behaviour of reinforced concrete bridge bent retrofitted with buckling restrained braces", Engineering Structures, Vol. 119, pp: 34–48.

[25] Hosseinzadeh, Sh., Mohebi, B. (2016). Seismic evaluation of all steel buckling restrained braces using finite element analysis", Journal of Constructional Steel Research, Vol. 119, pp: 76-84

[26] Khan, F. R., H. Iyengar, J. P. Colaco, (1966). Complete Design of the100-story John Hancock Centre" ASCE Journal of the Structural Davison, ST6, December, pp: 55-73

[27] ANSI/AISC360-10. (2005). American Institute for Steel Construction (AISC) Specification Structural Steel Buildings Chicago: American Institute for Steel Construction.

[28] PERFORM-3D. (2006). PERFORM-3D Nonlinear Analysis and Performance Assessment for 3D Structures: Computers and Structures, Inc. University Avenue Berkeley, California.

[29] FEMA356. (2000). FEDERAL EMERGENCY MANAGEMENT AGENCY (FEMA 356) Prestandard and Commentary for The Seismic Rehabilitation of Buildings. Virginia.

[30] Pan, T.C., Brownjohn, J.M.W., You, X.T. (2004). Correlating Measured and Simulated Dynamic Responses of a Tall Building to Long-Distance Earthquakes. Earthquake Engineering & Structural Dynamics, Vol. 33, pp: 611-632.

[31] ASCE/SEI41-13. (2014). American Society of Civil Engineers (ASCE/SEI 41-13) Seismic Evaluation and Retrofit of Existing Buildings. United States of America: American Society of Civil Engineers.